Article

JOURNAL OF COMPOSITE MATERIALS

Journal of Composite Materials
47(6–7) 805–825

DOI: 10.1177/0021998313476394
jcm.sagepub.com
SAGE

A comparison of experimental data with multicontinuum failure simulations of composite laminates subjected to tri-axial stresses

Andrew C Hansen[1], Emmett E Nelson[2] and Douglas J Kenik[2]

Abstract

This article presents progressive failure predictions, and comparisons against experimental data, for a variety of continuous fiber composite laminates subjected to multiaxial stress states. The work is part of a broader effort known as the Second World-Wide Failure Exercise. The emphasis of Second World-Wide Failure Exercise is a study of the influence of hydrostatic compressive stress on the stress–strain response and ultimate failure of the composite laminates studied. Polymers tend to exhibit significant increases in ultimate strength in the presence of hydrostatic compressive stresses. Nonlinear stress–strain behavior is also commonly observed. The complex material behavior of polymers presents several challenges in the analysis of composite materials where polymer resins are used as the matrix constituent. Failure simulations presented are multiscale in nature, consisting of a nonlinear finite element formulation with resolution extending down to the lamina level. The finite element analysis is further coupled to a multicontinuum theory where fiber and matrix constituents are treated as separate but linked continua. In general, the results of the multicontinuum theory failure simulations are in excellent agreement with the experimental data. The simulations were able to capture a variety of interesting material behaviors that are illuminated by the unique constituent level information provided in a multicontinuum theory analysis.

Keywords

Composite, failure, multicontinuum, tri-axial stress, multiscale, finite element

Introduction

This study addresses the progressive failure of continuous fiber composite laminates at the scale of interest of the structural analyst. The goal is to develop a progressive failure analysis capable of predicting the global response of a structure, while capturing the inelastic deformation mechanisms that lead to ultimate failure.

A natural scale to describe the inelastic response of a composite is through a continuum description of the fiber and matrix constituents that coexist within a lamina of a unidirectional (UD) or multidirectional laminate. Geometric scales larger than the constituent level, such as the lamina level, require one to smear the behavior of the fiber and matrix into a homogeneous material. Because high performance continuous fiber composites are composed of constituents with vastly different thermo-mechanical properties, smearing of the properties of the fiber and matrix may mask important information from the analyst. For instance, virtually all the inelastic deformation mechanisms leading to a nonlinear response prior to ultimate failure occur within the matrix constituent. It is clearly desirable to describe these *matrix* deformation mechanisms using *matrix* constituent stress and strain fields—free of the strong influence of fiber material properties.

Geometric scales smaller than the continuum description of the fiber and matrix constituents present an entirely different set of difficulties. To begin, one is immediately confronted with the challenge of modeling fiber distributions along with constituent flaws such as matrix voids. A statistical formulation, or some other averaging process of the microscale information, is necessary to bring the analysis back to a scale that is meaningful to the structural analyst. The process of averaging microstructural variables is simply an

[1]Department of Mechanical Engineering, University of Wyoming, USA
[2]Firehole Technologies, Inc., USA

Corresponding author:
Andrew C Hansen, Department of Mechanical Engineering, University of Wyoming, Laramie, WY 82071, USA.
Email: hansen@uwyo.edu

alternate form of the volume averaging that occurs naturally from a continuum perspective. Moreover, the microstructural averaging process comes with intense computational demands that are often numerically untenable.

Our approach to develop a progressive failure structural analysis for composite laminates using constituent information requires one to efficiently cross multiple geometric scales starting at the structural level. To begin, a finite element based analysis is utilized to bring stress/strain resolution from the laminate level down to the individual lamina. Embedded in the lamina analysis is a multicontinuum theory (MCT) algorithm that further decomposes lamina stress and strain fields down to the fiber and matrix constituent level stress/strain fields. Failure criteria are developed at the constituent level within a lamina and applied independently based on the stress fields seen by each constituent.

The present theory assumes linear elastic behavior of the fibers up to fiber failure. Inelastic behavior of the matrix is allowed, caused by a variety of deformation mechanisms forming sequentially from submicrocrack accumulation to macroscopic cracks such as transverse ply cracks (parallel to the fibers), and finally to complete matrix failure. The degree of matrix damage is tracked up through ultimate matrix failure with material properties continuously modified as damage accumulates. An important observation that is critical to the numerical efficiency of an MCT structural analysis is that the relationships between composite properties and damaged or failed constituent properties are completely determined prior to structural analysis.

This study is directed at predicting composite material failure for laminates subjected to a significant hydrostatic compressive stress state. Constituent (fiber and matrix) material stiffness constants are assumed to be independent of hydrostatic pressure. Fiber and matrix tensile strengths are also assumed to be independent of hydrostatic compressive stress. Compressive strengths are assumed to be linearly increasing functions of hydrostatic compressive stress.

Finally, a persistent question that routinely arises in failure simulations is the impact of residual cure stresses on failure predictions. We address this question in this study by first modeling the cure process to predict cure stresses and then studying the effects of these residual stresses on failure predictions for UD laminates.

Key features of the analysis

In what follows, we provide the salient features of the nonlinear multiscale analysis used in this Second World-Wide Failure Exercise (WWFE-II). The guidelines for the Exercise may be found in Kaddour and Hinton.[1] The reader is referred to our contribution to Part A of the Exercise for additional details on many of the topics discussed.[2]

Overview of MCT

The fundamental premise underlying continuum mechanics is that all physical quantities of interest represent average values of the quantity where the averaging occurs over a material volume whose physical dimensions are small compared to the physical dimensions of the system of interest, yet large enough to capture the average behavior. For instance, a continuum (material) point for a UD continuous fiber composite at the scale of the lamina is shown in Figure 1(a). The macroscopic value used to characterize the stress tensor at this point in a single continuum is derived by taking a volume average of all stresses as

$$\underset{\sim}{\sigma} = \frac{1}{V}\int_D \underset{\sim}{\sigma}\,(\mathbf{x})\,\mathrm{d}V \tag{1}$$

where the volume averaging occurs over both matrix and fiber constituents. Of course, the beauty of the continuum approach is that the integral volume average of equation (1) is never explicitly computed, as the volume-averaged stress on the left hand side (LHS) of equation (1) is taken as the primitive stress variable. In contrast, microscale formulations are forced to perform some type of volume averaging or statistical process to return to the scale of interest.

The concept of a multicontinuum simply extends the notion of a continuum to reflect coexisting materials within a continuum point. Such an extension is natural in any case where there are two, or more, clearly identifiable constituents with drastically different material properties. In particular, consider a continuous fiber composite material where the matrix (m) and fibers (f) are allowed to retain their identity in the continuum, as shown in Figure 1(b) and 1(c). Using equation (1) for each constituent, one can write

$$\underset{\sim}{\sigma}_f = \frac{1}{V_f}\int_{D_f} \underset{\sim}{\sigma}\,(\mathbf{x})\,\mathrm{d}V \tag{2}$$

and

$$\underset{\sim}{\sigma}_m = \frac{1}{V_m}\int_{D_m} \underset{\sim}{\sigma}\,(\mathbf{x})\,\mathrm{d}V \tag{3}$$

Again, the volume averaging in equations (2) and (3) is purely symbolic in nature as the continuum (averaged) forms of $\underset{\sim}{\sigma}_m$ and $\underset{\sim}{\sigma}_f$ are taken as the primitive variables. Combining equations (1) to (3) leads to

$$\underset{\sim}{\sigma} = \phi_f\,\underset{\sim}{\sigma}_f + \phi_m\,\underset{\sim}{\sigma}_m \tag{4}$$

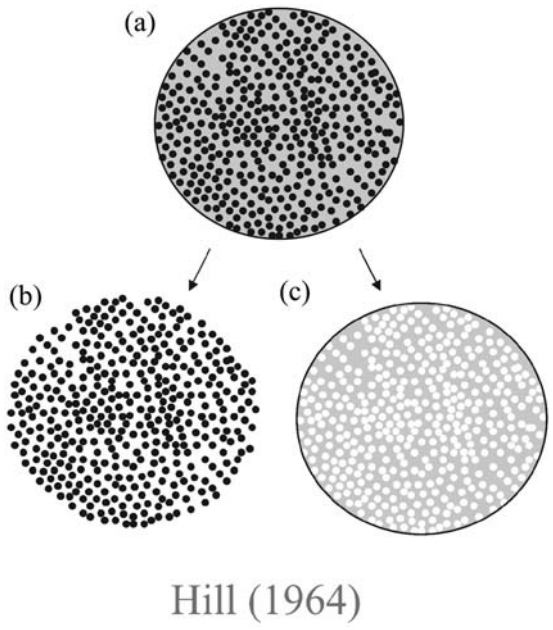

Figure 1. Multicontinuum decomposition schematic of: (a) a continuum (material) point for a UD continuous fiber composite at the scale of the lamina; (b) the same point showing only fibers; and (c) the same point showing only the matrix material.
UD: unidirectional.

where ϕ_f and ϕ_m are the volume fractions of fiber and matrix, respectively. Likewise, for strains

$$\underset{\sim}{\varepsilon} = \phi_f \underset{\sim}{\varepsilon}_f + \phi_m \underset{\sim}{\varepsilon}_m \tag{5}$$

The ability to decompose lamina level continuum fields to the constituent level requires a relationship between composite and constituent elastic constants. The link between material properties is accomplished using a finite element micromechanics model of a representative composite microstructure.

The choice of microstructure to model is entirely up to the analyst and fully random microstructures that are truly representative of actual composite microstructures may be utilized. This study utilized a periodic fiber arrangement based on hexagonal packing. Recently, Anderson[3] has performed a significant study comparing material properties of random microstructures versus ordered structures such as hexagonal fiber packing. Regardless of the microstructure chosen, the necessary micromechanical solutions are decoupled from the nonlinear structural solution, thereby allowing the user to model microstructures to any degree of accuracy desired without impacting structural solution times.

Given the necessary preprocessed information from micromechanics analysis, access to constituent level multicontinuum information comes with virtually no computational burden compared to that of a single continuum formulation at the lamina level. However, the additional information generated can be significant. Perhaps, the best demonstration of the value of constituent information is a study of free thermal expansion/contraction of a UD laminate. For instance, as the temperature of a free composite plate is lowered from a reference state, the composite is free to contract and the laminate remains in a stress-free state. However, due to mismatched constituent thermal expansions between the fiber and the matrix, large self-equilibrating thermally induced stresses develop in each constituent. The multicontinuum analysis described herein faithfully captures the internal stress states seen by each constituent. These stresses can become so large that matrix cracking can occur in carbon/epoxy materials cooled down to cryogenic temperatures.

Constituent level failure criteria

The microstructure of a UD continuous fiber lamina introduces interesting complexities in a failure analysis that are intrinsic to the scale of the fiber and matrix constituents. In particular, if one were to consider the matrix material with the fibers removed, the matrix may be thought of as a block of 'Swiss cheese', as shown in Figure 2. The immediate conclusion regarding macroscopic (lamina level) behavior is that failure of the matrix constituent is anisotropic as transverse tensile failure levels will clearly be different than longitudinal tensile failure.

In what follows, failure of both the fiber and matrix constituents is assumed to satisfy transverse isotropy. Therefore, we develop stress-based failure criteria based on the transversely isotropic invariants given by

$$\begin{aligned} I_{1\beta} &= \sigma_{11\beta} \\ I_{2\beta} &= \sigma_{22\beta} + \sigma_{33\beta} \\ I_{3\beta} &= \sigma_{22\beta}^2 + \sigma_{33\beta}^2 + 2\sigma_{23\beta}^2 \\ I_{4\beta} &= \sigma_{12\beta}^2 + \sigma_{13\beta}^2 \\ I_{5\beta} &= \sigma_{22\beta}\sigma_{12\beta}^2 + \sigma_{33\beta}\sigma_{13\beta}^2 + 2\sigma_{12\beta}\sigma_{13\beta}\sigma_{23\beta} \end{aligned} \tag{6}$$

where the subscript β represents fiber (f) or matrix (m), depending on the constituent of interest.

A matrix failure within a UD lamina utilized by Mayes and Hansen[4] in a contribution to the First World-Wide Failure Exercise (WWFE-I) is given by

$$^{\pm}A_{3m} I_{3m} + A_{4m} I_{4m} = 1 \tag{7}$$

where the invariants are based on the matrix stresses.

The A_{jm} in equation (7) are constituent failure parameters generally derived from experimentally determined composite ultimate strength data through correlation with the MCT decomposition. The $\pm$ sign

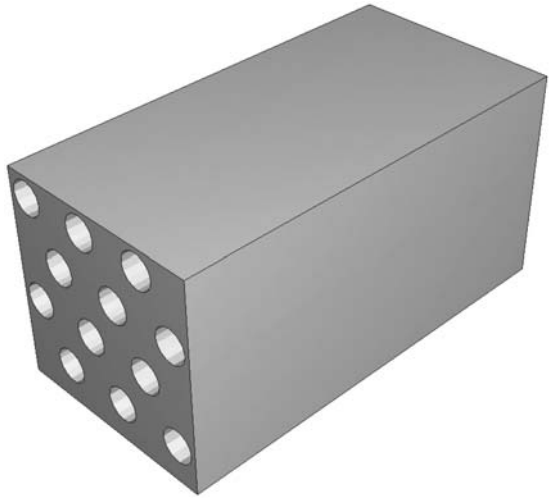

Figure 2. Schematic of the matrix material of a continuous fiber composite with the fibers removed.

in equation (7) indicates a dependence of the parameter on tensile versus compressive stresses.

An important property of the matrix failure criterion shown in equation (7) is that it lacks the presence of σ_{11m}. The absence of σ_{11m} was noted as a potential deficiency in the matrix failure criterion for glass/epoxy composites in our contribution to Part A of the Exercise.[2] To correct this situation, we introduced the following quadratic matrix failure criterion given by

$$^{\pm}A_{1m}I_{1m}^2 - {}^{\pm}A_{2m}I_{2m}^2 + A_{3m}I_{3m} + A_{4m}I_{4m} - {}^{\pm}A_{5m}I_{1m}I_{2m} = 1 \quad (8)$$

The motivation for introducing terms A_{1m}, A_{2m}, and A_{5m} in equation (8) is that the criterion collapses to a von Mises yield surface for an isotropic material.

Mayes and Hansen[4] developed a fiber failure criterion to detect fiber failure within a lamina given by

$$^{\pm}A_{1f}I_{1f}^2 + A_{4f}I_{4f} = 1 \quad (9)$$

where the invariants are as defined in equation (6) using fiber stresses.

For the present Exercise, we elected to leave the fiber failure criterion of equation (9) unaltered. However, evidence from data presented by the organizers suggests that additional terms similar to those found in the matrix criterion may be useful. Also, biaxial cruciform data generated at Air Force Research Laboratory (Personal communication, Jeffrey Welsh, Operationally Responsive Space Office.) suggests that a more interactive fiber failure criterion should be examined. Of particular interest are terms involving I_{2f} to accommodate the effects of transverse compression on fiber failure. Examples of structural loads where such a modification may be beneficial are found in Cases 10 and 11.

A major aspect of the theoretical development of the constituent failure criteria is the determination of the various failure coefficients in equations (8) and (9). The process for determining these coefficients is detailed in our contribution to Part A of the Exercise.[2]

Inelastic matrix behavior

As noted previously, we adopt the position that nonlinear behavior of a composite is attributed entirely to inelastic behavior in the matrix constituent as the fiber is assumed linear elastic to failure. Damage in the matrix is manifested in the form of several deformation mechanisms including submicrocrack (molecular bond rupture) accumulation to formation of macroscopic transverse ply cracks of increasing crack densities. In the analyses presented here, we identify three separate regimes of inelastic deformation in the matrix given by: (a) pre-failure, (b) initial matrix failure, and (c) matrix saturation. The reader is referred to our contribution to Part A of the Exercise[2] for a detailed discussion of this progression of inelastic deformation. A brief description of our terminology for observed inelastic deformation is given as follows.

1. *Pre-failure*: Nonlinearity is introduced through submicrocrack accumulation. This nonlinearity is allowed in transverse compression and longitudinal and transverse shear.
2. *Initial matrix failure*: This value represents the onset of a transverse matrix crack leading to failure of a *UD* composite under transverse tension. Also, in the case of through-thickness tension for any laminate configuration, initial matrix failure is assumed to cause ultimate failure of the specimen.
3. *Matrix saturation*: This term represents a maximum value of transverse crack saturation at which point the matrix has lost a substantial portion of its load-carrying capacity. Matrix crack saturation can only occur in in-plane loading of multidirectional laminates, where a composite can continue to sustain load after an initial transverse crack. Knops and Bögle[5] provide a very fine study of growth in transverse crack density of cross-ply laminates.

In the present MCT failure analysis, pre-failure material nonlinearity, such as that typically seen in longitudinal shear and transverse normal compression, is modeled as follows. Material degradation is driven by the compressive normal and longitudinal shear contributions to the matrix failure criterion, as presented in equation (8). For the purpose of discussion, one can

rewrite this equation, using compression parameters $^{-}A_{jm}$, as

$$\eta_{Nm} + \eta_{Sm} = 1 \tag{10}$$

where

$$\eta_{Nm} = {}^{-}A_{1m}I_{1m}^2 - {}^{-}A_{2m}I_{2m}^2 + A_{3m}I_{3m} - {}^{\pm}A_{5m}I_{1m}I_{2m} \tag{11}$$

and

$$\eta_{Sm} = A_{4m}I_{4m} \tag{12}$$

The composite longitudinal shear modulus, G_{12}, and normal moduli, E_{22} and E_{33}, are degraded as functions of η_{Sm} and η_{Nm}, respectively. The degradation curves are taken from longitudinal shear and uniaxial transverse compression data. Moreover, the nonlinear response for transverse compression is also used to define the through-thickness compression behavior.

Anytime composite properties are altered due to matrix damage, the properties of the matrix material must also be degraded in order to maintain consistent relationships through the micromechanics analysis. This consistency is enforced a priori to structural analysis by generating composite material property curves as a function of matrix damage. It is a straightforward matter to relate degraded composite properties to degraded matrix properties as functions of simple curves for any composite material. It should be noted that the matrix is allowed to degrade as a transversely isotropic material, thereby decoupling longitudinal shear nonlinear behavior from compressive nonlinear behavior.

The development begins with isotropic matrix material properties, say E_m and G_m, representing Young's modulus and the shear modulus, respectively. Modulus G_m is allowed to degrade in longitudinal shear to $G'_{12m} = G'_{13m}$. Similarly, Young's modulus, E_m, degrades to $E'_{11m} = E'_{22m} = E'_{33m}$. Therefore, the nonlinear response for transverse compression is assumed to be identical to the nonlinear response for through-thickness compression behavior.

Transverse isotropy of the in-plane matrix shear modulus is also enforced leading to

$$G'_{23m} = \frac{E'_{22m}}{2(1 + \nu_{23m})} \tag{13}$$

where Poisson's ratio is held constant.

A post-failure degradation model was also developed to account for a gradual reduction in failed matrix material properties in multidirectional laminates. The model is intended to capture the material response of a point in a lamina, which is part of a *multidirectional* laminate, after a matrix failure is predicted. However, in the case of *UD* laminates, constituent material properties are zeroed when matrix failure is detected—an approach consistent with the work of Mayes and Hansen.[6,7] The reader is referred to our contribution to Part A of the Exercise[2] for the detailed development of the post-failure response.

Finally, ultimate failure is determined, if it occurs at all, by the first fiber failure in any ply of a multidirectional laminate. Fiber failure produces significant reductions in stiffness and an associated drop-off in load for a displacement controlled analysis—or a jump in displacement in a load-controlled analysis. In the case of a *UD* composite, final failure is determined by either initial matrix failure or fiber failure.

Hydrostatic stress effects

A review of the effects of hydrostatic stress on the mechanical behavior of polymers and polymer-based composites is given by Hoppel et al.[8] In general, many polymers tend to show an increase in modulus and strength as a function of increasing hydrostatic pressure, p, defined herein as one-third the trace of the stress tensor, i.e.

$$p = -\frac{1}{3}(\sigma_{11} + \sigma_{22} + \sigma_{33}) \tag{14}$$

In this study, we have chosen not to alter the elastic material properties in the presence of hydrostatic pressure. Tensile strengths were also assumed to be independent of hydrostatic stress.

In contrast to tensile strengths, the effect of pressure on polymer compressive strengths is believed to be substantial. Based on the literature review provided by Hoppel et al.,[8] matrix compressive strengths are assumed to be linear increasing functions of hydrostatic compressive stress. Moreover, fiber compressive strengths are also assumed to be linear increasing functions of hydrostatic compressive stress. The rationale for increasing fiber strengths under pressure is based on the premise that fiber failure in longitudinal compression is actually initiated by matrix failure mechanisms, resulting in instabilities causing fiber kinking and/or buckling. Wronski and Parry[9] and Parry and Wronski[10] provide experimental evidence combined with analytical models to support the notion of matrix failure leading to fiber failure in compression. The often observed, substantially lower, failure strengths of UD composites in compression versus tension provide additional qualitative evidence to support this view.

Our approach to reasonably determine the effect of hydrostatic pressure on polymer matrix strengths was to examine neat resin data from Hine et al.[11] We begin by assuming a quadratic, isotropic failure criterion in principal stress space where different failure levels may be accounted for through the leading coefficient $\pm A$.

$$\pm A(\sigma_{11}-\sigma_{22})^2+\pm A(\sigma_{11}-\sigma_{33})^2+\pm A(\sigma_{22}-\sigma_{33})^2=1 \tag{15}$$

The positive or negative value of A is chosen based on the sign of the first invariant (trace) of the stress tensor. A von Mises failure envelope is recovered by forcing $\pm A$ to be identical in tension and compression. An alternative approach to account for different tensile and compressive strengths is to introduce linear stress terms in the failure criterion, again through the first invariant.[12]

Coefficient $\pm A$ is determined from uniaxial tension/compression data as

$$\pm A=\frac{1}{(\pm\sigma_u)^2} \tag{16}$$

where $\pm\sigma_u$ represents the ultimate stress in tension and compression, respectively.

Neat resin polymer compressive strength, $^{-}\sigma_u$, as used in equation (16), is further assumed to be a linear function of hydrostatic stress. Specifically, the form of matrix strength hardening under hydrostatic compressive stress is assumed to be

$$^{-}\sigma_u={}^{-}\sigma_u^o+C\left(\sigma_{kk}-1.1\,\sigma_{kk}^*\right) \tag{17}$$

where σ_{kk} represents the trace of the stress tensor and σ_{kk}^* a threshold value of hydrostatic stress defined by the value of σ_{kk} at failure in uniaxial compression. In particular, under the one-dimensional stress state of uniaxial compression

$$\sigma_{kk}^*={}^{-}\sigma_u \tag{18}$$

If the hydrostatic stress, σ_{kk}, is below the threshold value of $1.1\ \sigma_{kk}^*$, the hardening of equation (17) is not invoked. The threshold value of σ_{kk}^* was chosen to eliminate a hardening effect under pure uniaxial compression. The multiplier of 1.1 is a numerical convenience introduced to insure that the hydrostatic stress truly cleared the threshold stress before hardening begins. Based on data provided by Hine et al.,[11] the coefficient, C, of equation (17) was determined to be 0.04. It should be noted that the value $C=0.04$ was utilized as the hardening parameter for the matrix constituent in the analysis of all cases in the present Exercise.

Strength hardening of the matrix material within a composite is assumed to be isotropic in the sense that all strength parameters in equation (8) are increased proportionally under hydrostatic compressive stress. Because parameter A_{4m} is readily isolated from other strength parameters, we have chosen to harden this parameter as follows.

$$A_{4m}=\frac{1}{(S_{12m})^2} \tag{19}$$

where following equation (17), matrix strengths, S_{12m}, are assumed to take the form

$$S_{12m}=S_{12m}^0-0.04\left(\sigma_{kkm}-1.1\,\sigma_{kkm}^*\right) \tag{20}$$

The threshold hydrostatic stress, σ_{kkm}^*, for the matrix material is computed from the matrix stress state at failure in uniaxial transverse compression. Isotropic (proportional) strengthening is imposed by modifying all other compressive parameters of equation (8) as

$$A_{jm}=A_{jm}^o\left(\frac{A_{4m}}{A_{4m}^o}\right) \tag{21}$$

where A_{jm}^o denotes failure parameters in the absence of hydrostatic pressure.

A similar procedure is followed to introduce fiber strengthening in the presence of transverse compression in the *matrix* defined by $I_{2m}<0$. As noted previously, the apparent failure properties of fibers in compression in a UD composite are attributed to matrix failure mechanisms that lead to fiber kinking and/or buckling. Based on this premise, we chose to strengthen fiber properties in compression in identical proportion to those of the matrix. Specifically, we assume

$$A_{jf}=A_{jf}^o\left(\frac{A_{4m}}{A_{4m}^o}\right) \tag{22}$$

where, again, hardening only occurs if the matrix pressure is above the threshold value defined in equation (20). Our approach to specifying fiber hardening to be proportional to the matrix strength hardening is admittedly simplistic and the topic warrants substantial additional research. The approach taken here is believed to be a reasonable starting point to address these complex phenomena.

The effect of thermally induced cure stresses

Our current approach to determine constituent-based failure in an MCT analysis relies on the assumption that both the fiber and matrix are at a stress-free state before loading. This assumption is based on the premise

that any residual cure stresses residing in the constituents before a strength test are accounted for during the strength test and the resulting strength parameters intrinsically account for the cure stresses. In other words, if failure strength of a composite at ambient temperature was decomposed to the fiber and matrix, the measured constituent failure strengths would include the effects of the cure cycle. While this argument is both elegant and desirable from an implementation perspective, the question of thermal cure stresses affecting failure of composites presents itself as a viable and somewhat problematic possibility.

To address the effect of cure stresses on failure predictions, Kenik[13] performed a detailed study of failure envelope predictions for UD composite laminates. Both glass/epoxy and carbon/epoxy materials were studied. The matrix material chosen for the study was Derakane 510, a vinylester polymeric resin supplied by the Naval Surface Warfare Center and manufactured by Dow®. This specific resin was chosen because its material properties at elevated temperatures are well characterized.[14] The resin was modeled as a linear viscoelastic material with time–temperature superposition (TTS) with several different cool down cycles. Self-equilibrating matrix and fiber cure stresses were determined and these stresses were then accounted for in making failure envelope comparisons. We emphasize that the constituent strength coefficients must be re-derived to account for the influence of the residual cure stresses. For instance, in a purely mechanical problem, matrix failure coefficient ${}^{+}A_{1m}$ is determined as

$$ {}^{+}A_{1m} = \left(\frac{1}{({}^{+}S_{11m})^2} \right) \tag{23} $$

where ${}^{+}S_{11m}$ represents the longitudinal stress in the matrix at composite longitudinal tensile failure. In contrast, when incorporating the effects of the cure cycle, coefficient ${}^{+}A_{1m}$ is computed as

$$ {}^{+}A_{1m} = \left(\frac{1}{\left({}^{+}S_{11m} + \sigma_{11m}^{(cure)} \right)^2} \right) \tag{24} $$

Here, ${}^{+}S_{11m}$ is the experimentally computed matrix stress at composite longitudinal tensile failure and $\sigma_{11m}^{(cure)}$ the longitudinal stress in the matrix resulting from the cure cycle.

In WWFE-I, the first three failure envelope predictions requested by the organizers were for UD laminates.[15] In particular, Case 1 was for a glass/epoxy UD lamina loaded under longitudinal shear and transverse tension/compression. Using this load case as a reference for the present glass/epoxy studied by Kenik,[13] failure envelopes were generated with and without residual stresses to determine the effects of cure stresses on failure. Figure 3 depicts the failure envelope comparison. The two failure envelopes are, for practical purposes, identical, thereby indicating that cure stresses are intrinsically accounted for by the failure data generated at ambient temperature. It should be noted that Kenik's[13] study showed *residual cure stresses did alter*

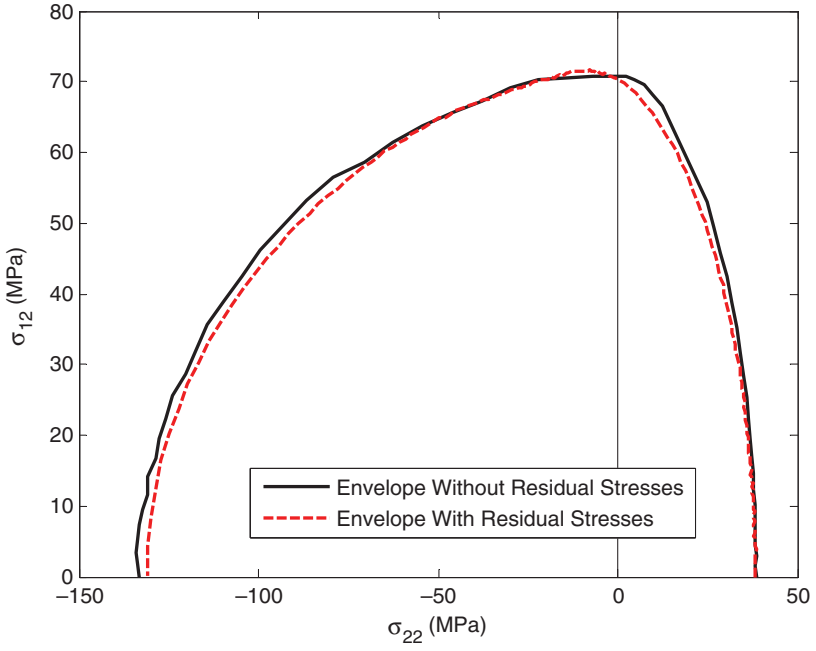

Figure 3. Failure envelop comparison of a glass/epoxy composite under combined longitudinal shear and transverse tension/compression for the cases with and without residual cure stresses.

failure predictions for laminates tested at temperatures away from room ambient temperatures.

The importance of thermal stresses arising from large temperature differences is also of interest in multidirectional laminates. Such a study requires a multicontinuum formulation with viscoelastic TTS, a capability that is currently not available. Hence, any definitive statements about the effects of cure stresses on failure predictions of multidirectional laminates cannot be made. In the absence of the ability to model cure stress effects using a TTS viscoelastic analysis for multidirectional laminates, we adopt the assumption of a stress-free state at room temperature.

Material property discussion

A fundamental requirement of an MCT analysis is to enforce a consistent set of composite and constituent material properties through the finite element micromechanics model. Generally speaking, the bulk material properties of the constituent materials used in the micromechanics model may *not* yield accurate homogenized composite properties when compared to experimental data. There are several reasons that can cause this discrepancy.

1. Some bulk elastic properties of fibers, particularly shear and transverse normal values, are generally not accurately known and are inferred from composite data.
2. The general difficulties in experimental testing of some composite properties may lead to further discrepancies.
3. The micromechanical finite element model represents an idealized microstructure, not the actual microstructure.
4. Knowledge of the mechanical properties of the fiber/matrix interphase is lacking.

Given a set of constituent and composite properties, one is immediately faced with the challenge of reconciling any inconsistencies based on the micromechanics model chosen. Our primary goal is to reproduce the composite properties as accurately as possible. The in situ fiber and matrix properties are adjusted, within reason, to best fit the homogenized composite properties as measured.

A discussion of the development of a consistent set of matrix, fiber, and composite properties may be found in our contribution to Part A of the Exercise.[2] Tabular data of constituent and composite elastic constants are provided.

With the exception of transverse shear strengths, all composite strength data are identical to that provided by the organizers. Transverse shear strengths were increased to values above those of the organizers but were held below values provided for longitudinal shear strengths. Our motivation for increasing the transverse strength surrounds the ability to maintain transverse isotropy of the matrix failure criteria while enforcing the constraint that matrix failure is independent of hydrostatic stress states. An additional rationale for increasing transverse shear strengths is our belief that the reported transverse shear strengths reflect a delamination failure rather than a true material failure within a lamina. Table 1 presents the revised transverse shear strengths used in the analysis compared with the original transverse shear strengths supplied in the Exercise.

Numerical implementation

The MCT failure algorithm described herein was implemented in the commercial nonlinear finite element code *ABAQUS Standard*. An '*ABAQUS umat*', a user-defined subroutine, was added to the *ABAQUS* program to achieve the MCT decomposition. Loading to failure was performed incrementally with *ABAQUS* default convergence parameters for nonlinear iteration. Load control was used for all analyses presented and no convergence difficulties were encountered. Additional information on the numerical implementation may be found in our contribution to Part A of the Exercise.[2]

Results

In what follows, MCT predictions for the 12 cases requested by the organizers are presented along with the data provided by the organizers after the submission of Part A. The numerical results generated are not altered from our original submission of Part A of the Exercise.[2]

An important feature of the nonlinear analysis used to produce our predictions is that pre-failure and post-

Table 1. Original and adjusted composite transverse shear strengths.

(MPa)	IM7/8551-7	T300/PR319	AS/epoxy1	E-glass/MY750	S2/epoxy2
Given S23	57	45	50	40	50
Adjusted S23	82	64	72	46	74

failure nonlinear behavior was accounted for in longitudinal shear. However, only post-failure nonlinear behavior was implemented for transverse and through-thickness compression. Pre-failure nonlinear behavior is believed to be important for modeling nonlinear compressive stress–strain behavior. Our lack of modeling pre-failure nonlinearity in compression is attributed to code limitations at the time of our submission[2] of Part A of the Exercise.

Case 1

The first test case involves predicting the failure envelope of MY750 epoxy as a neat resin when subject to superposed hydrostatic pressure. This problem involves a single constituent only and, as such, it does not require a multicontinuum analysis. Figure 4 shows the predicted failure envelope requested under hydrostatic stress. Matrix failure is based on a von Mises type failure criterion where different failure strengths are allowed in compression and tension. Matrix strengthening is evident in the compressive zone due to the hydrostatic pressure. The specific form of matrix strengthening is given in equation (17). The failure envelope does not close on or near the hydrostatic stress line as a von Mises surface is independent of hydrostatic stress.

The failure predictions are in excellent agreement with the reported experimental strengths taken from Hine et al.[11] This result should come as no surprise as the hardening coefficient used to define the hydrostatic strengthening was taken directly from their work. However, it is significant to note that the same matrix hardening coefficient was used in the remaining 11 cases.

The neat resin failure envelope shown in Figure 4 does not close on or near the hydrostatic stress line in tension as well. This phenomenon is consistent with a von Mises failure theory and is the result here of our matrix failure model given by equation (15). Clearly, failure in the tension zone will occur and, indeed, at relatively low stress levels. The present failure criterion would have to be modified if one were interested in modeling failure due to hydrostatic tensile stresses. For instance, a maximum stress criterion could be implemented in the tensile zone without affecting the results in the compressive region. Figure 5 shows this maximum stress tensile failure envelope with the expected closure in the tensile zone. Alternatively, one could introduce linear stress terms in the failure criterion to obtain closure under hydrostatic tension and compression.[12]

An important point to recognize here is that while the failure envelope of the neat resin is representative of

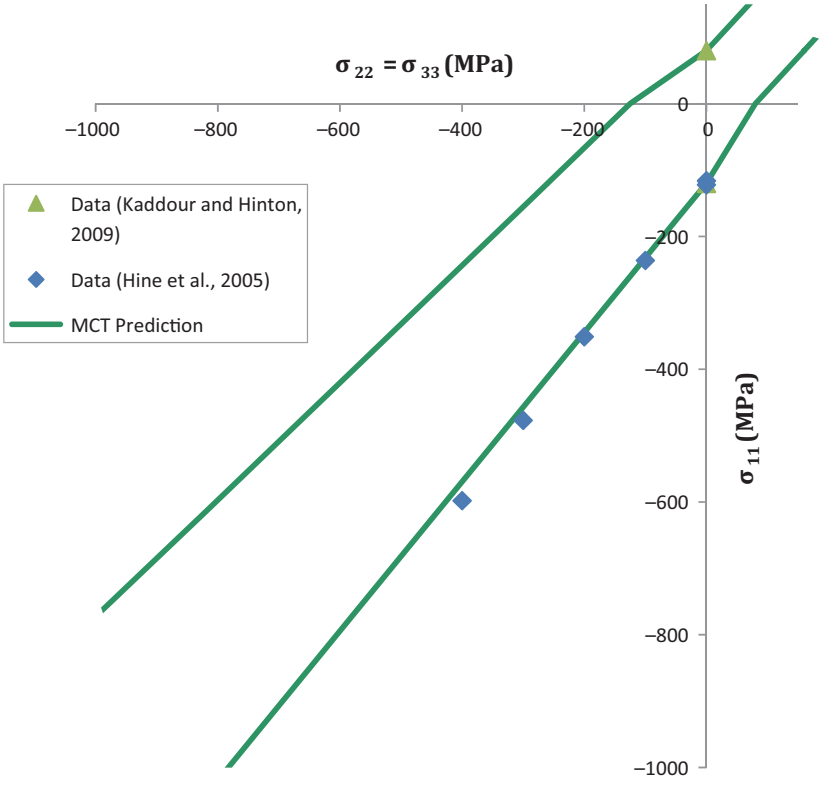

Figure 4. Test case 1; biaxial (σ_{xx} versus σ_{zz} with $\sigma_{yy} = \sigma_{zz}$) failure envelope prediction for MY750 epoxy with experimental data from Hine et al.[11]

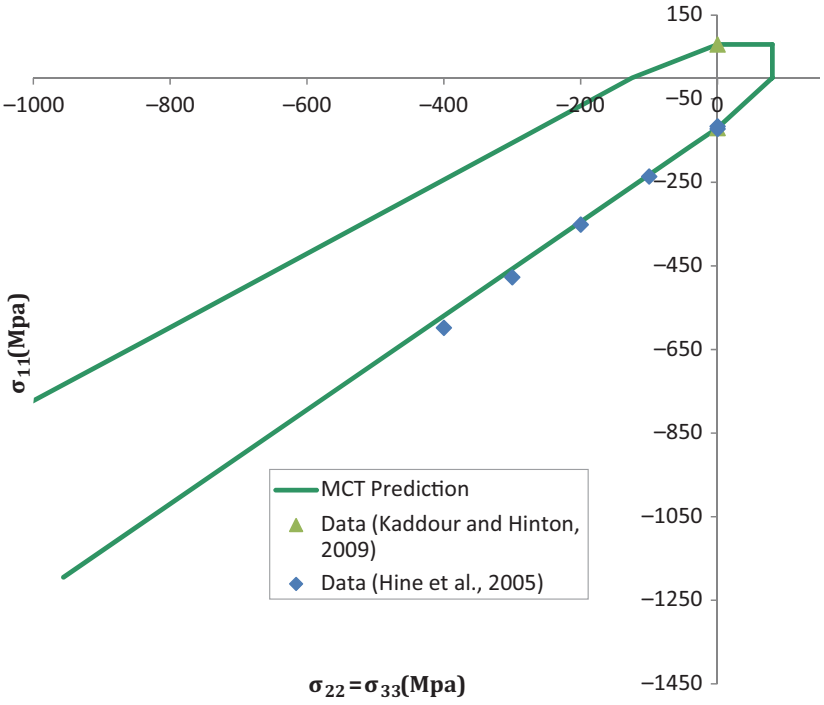

Figure 5. Test case 1; biaxial (σ_{xx} versus σ_{zy} with $\sigma_{yy} = \sigma_{zz}$) failure envelope prediction for MY750 modified to incorporate a maximum stress criterion in the tensile regime of quadrant I.

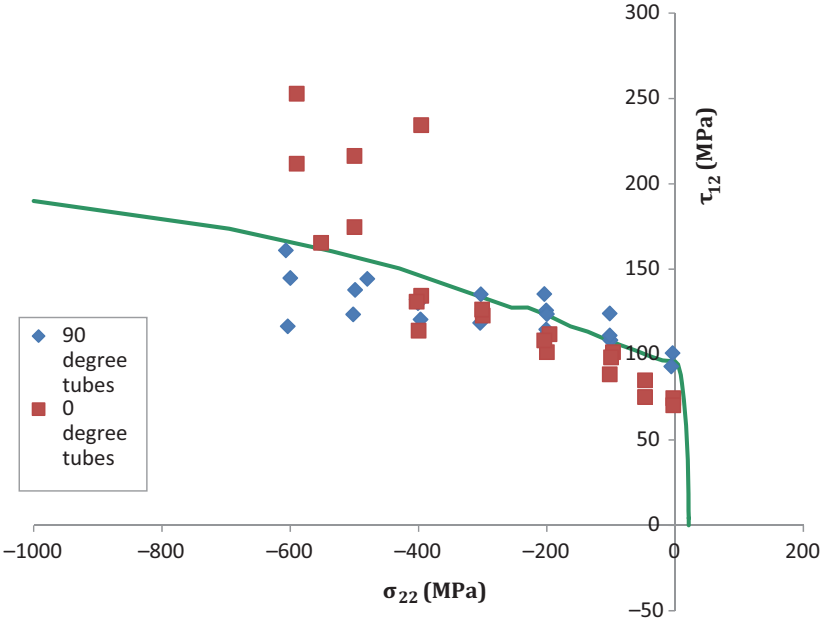

Figure 6. Test case 2; biaxial (τ_{12} versus σ_{22} with $\sigma_{11} = \sigma_{22} = \sigma_{33}$) failure envelope prediction for T300/PR319 graphite/epoxy UD laminate with experimental data from Shin and Pae.[16,17]
UD: unidirectional.

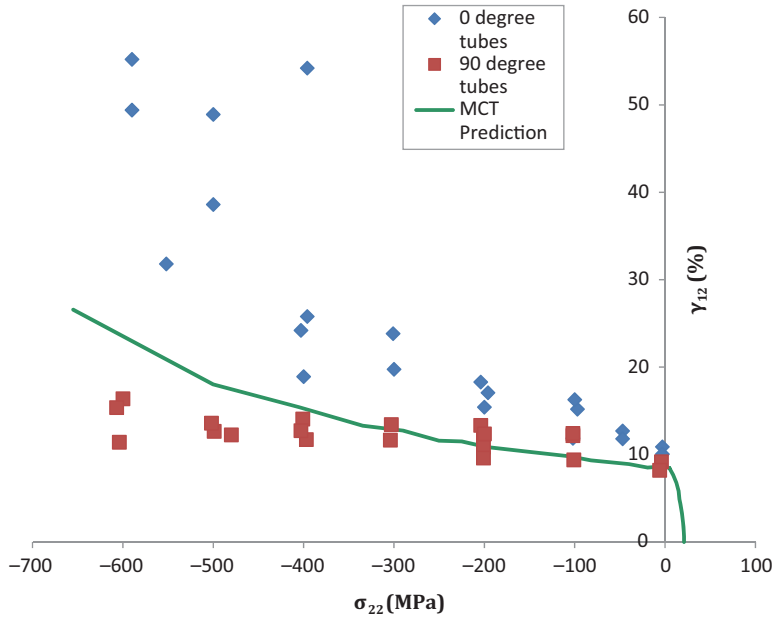

Figure 7. Test case 3; biaxial (γ_{12} versus σ_{22} with $\sigma_{11}=\sigma_{22}=\sigma_{33}$) failure envelope prediction for T300/PR319 graphite/epoxy UD laminate with experimental data from Shin and Pae.[16,17]
UD: unidirectional.

the trend of matrix behavior in a composite, a direct correlation with matrix failure envelopes in composite laminates is not possible. The reason is that matrix failure in a UD lamina is based on a *transversely* isotropic model which is the direct result of the microstructure of the matrix material at the lamina level.

Case 2

Figure 6 shows a predicted biaxial, τ_{12} versus σ_{22} with $\sigma_{11}=\sigma_{22}=\sigma_{33}$, failure envelope for a T300/PR319 graphite/epoxy UD laminate. Failure in quadrant I is driven by a combination of matrix tensile and matrix shear stresses. Failure in quadrant II is governed by matrix shear failure. Strengthening of the matrix due to hydrostatic pressure is readily apparent as the absence of this strengthening would produce a near horizontal failure prediction at 97 MPa in quadrant II, which is the pure shear value provided. The specific form of the strengthening is the result of the influence of hydrostatic stress on the failure parameters identified in equations (19) to (22). The correlation with the experimental data provided is excellent.

MCT does not predict constituent level failure under pure hydrostatic pressure and this is consistent with the predictions made in Test cases 5–8 described later. We believe there is merit in exploring a fiber failure criterion similar to the matrix criterion of equation (9) for very high stress levels. In this case, transverse fiber stresses may have an impact on failure loads.

Finally, the T300/PR319 composite is the one graphite/epoxy composite studied where we chose not to match the composite data as closely as possible. In particular, we chose to use a longitudinal shear modulus of 15 GPa for the graphite which is consistent with the value provided by the organizers. In order to match the composite longitudinal shear modulus, a fiber shear modulus of 2.4 GPa is required. This value is far below the shear modulus fibers for data from other carbon fibers. Matching the composite data precisely produces a similar response, as seen in Figure 4, but with a slightly lower slope with increasing compressive stress.

Case 3

Figure 7 shows a predicted biaxial stress–strain failure envelope of γ_{12} versus σ_{22} with $\sigma_{11}=\sigma_{22}=\sigma_{33}$, for the same T300/PR319 graphite/epoxy UD laminate of *Case 2*. Nonlinearities in the shear stress–strain response are attributed to the nonlinear shear behavior of the matrix material within the composite. We note that in all simulations presented herein, nonlinear shear stress–strain behavior is assumed independent of hydrostatic effects with the exception of ultimate failure. As in Case 2, the correlation with experimental data is very strong.

Case 4

Figure 8 shows the predicted stress–strain response in longitudinal shear for a T300/PR319 carbon/epoxy UD

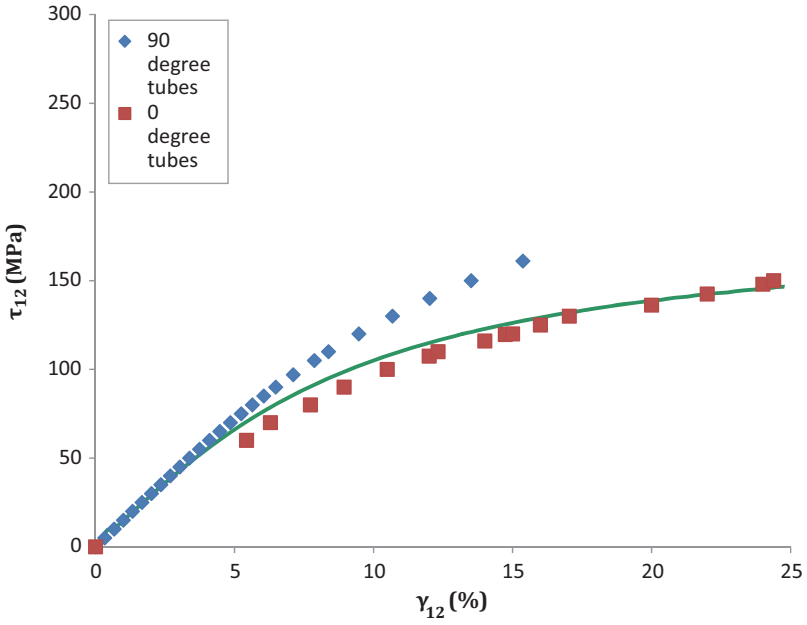

Figure 8. Test case 4; shear stress–strain curve (τ_{12} versus γ_{12} with $\sigma_{11}=\sigma_{22}=\sigma_{33}$) predictions for T300/PR319 graphite/epoxy UD laminate with experimental data from Shin and Pae.[16,17]
UD: unidirectional.

laminate *after* a 600 MPa hydrostatic stress has been applied. As noted previously, nonlinear stress–strain behavior is independent of hydrostatic pressure in this analysis. Hence, with the exception of an increase in the ultimate failure load, the nonlinear effects predicted here would be similar to the nonlinear response seen in the absence of hydrostatic compressive stress. The correlation with experimental data is excellent with the analytical predictions generally falling between the test data for the 0° and 90° tubes tested. The analysis and data presented were cut off at 25% strain, a value well in excess of any expected structural application.

Case 5

Figure 9 shows a predicted biaxial failure envelop, σ_{22} versus σ_{33} with $\sigma_{11}=\sigma_{33}$, for an E-glass/MY750 epoxy. Matrix failure governs the composite failure in all four quadrants. The predicted failure envelope in compression shows strong similarities to the neat resin matrix failure envelope shown in Figure 4. The excellent correlation with the data is not surprising given the strong influence of the matrix on transverse compressive failure and our ability to accurately model neat resin failure as seen in *Case 1* (Figure 4).

Case 6

Figure 10 shows a predicted biaxial failure envelop, σ_{11} versus σ_{33} with $\sigma_{22}=\sigma_{33}$, for an S-glass/epoxy2 UD composite. Quadrants I and II are governed by matrix failure, whereas quadrants III and IV are governed by fiber failure. The strengthening effect in compression in quadrant III is primarily attributed to matrix hardening and the accompanying fiber strengthening in compression. The bilinear behavior seen in quadrant III is the result of introducing hardening only after a threshold hydrostatic stress has been reached in the matrix material. For instance, in uniaxial compression in the x_1 (fiber) direction, the matrix stress state at failure is given by

$$[\sigma_m] = \begin{bmatrix} -52 & 0 & 0 \\ 0 & -3.1 & 0 \\ 0 & 0 & -3.1 \end{bmatrix} \text{MPa} \qquad (25)$$

The trace of the matrix stress at failure at failure is given by −58 MPa which is well below the threshold stress of −202 MPa, as determined from transverse compression data. As transverse compressive stress begins to build in the matrix, the hardening law for the matrix and fibers will kick-in at the critical value causing the bilinear response seen in quadrant III of Figure 10.

For this study, the ultimate fiber strength in tension is assumed to be constant and, furthermore, the fiber failure criterion is independent of transverse fiber stresses. At first blush, these factors would suggest that failure in quadrant I should be a vertical line,

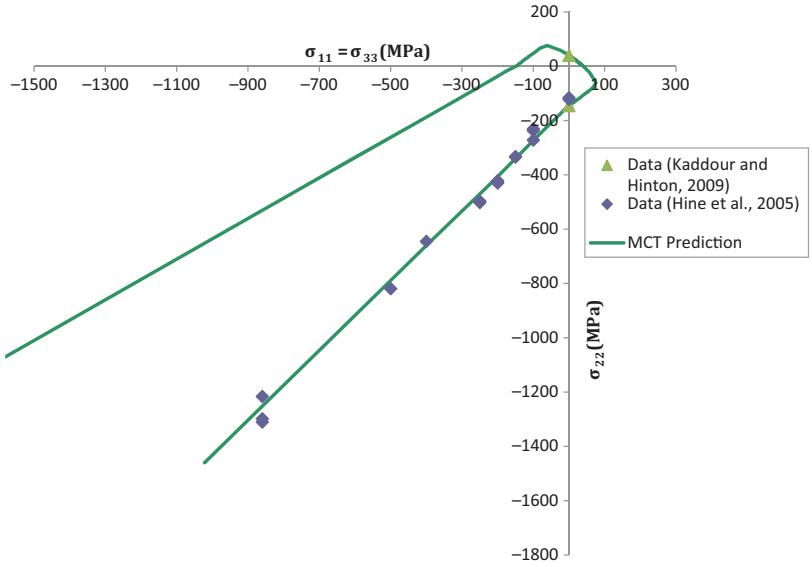

Figure 9. Test case 5; biaxial (σ_{22} versus σ_{33} with $\sigma_{11} = \sigma_{33}$) failure envelope prediction for E-glass/MY750 epoxy UD laminate with experimental data from Hine et al.[11]
UD: unidirectional.

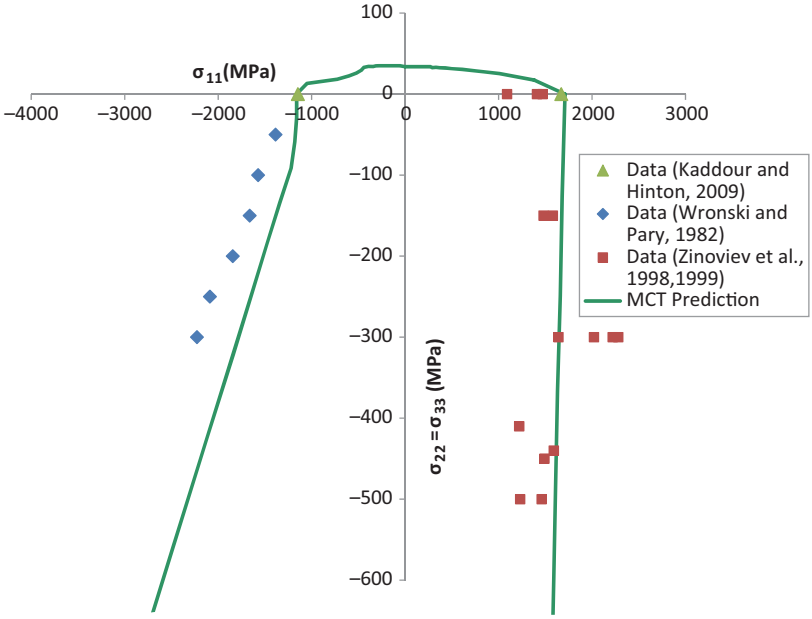

Figure 10. Test case 6; biaxial (σ_{11} versus σ_{33} with $\sigma_{22} = \sigma_{33}$) failure envelope prediction for S-glass/epoxy2 UD laminate with experimental data from Zinoviev and Tsvetkov,[18] Zinoviev et al.,[19] and Wronski and Parry.[9]
UD: unidirectional.

i.e. σ_{11f} = constant. However, the MCT prediction of the failure envelope shows that the tensile strength is decreasing with increasing composite transverse stresses in x_2 and x_3 directions. This phenomenon is entirely due to the MCT decomposition and is demonstrated by the fiber stress state shown in equation (26), which is the result of a biaxial composite compressive stress of $\sigma_{22} = \sigma_{33} = 10$ MPa.

$$\left[\sigma_f\right] = \begin{bmatrix} 4.29 & 0 & 0 \\ 0 & -10.8 & 0 \\ 0 & 0 & -10.8 \end{bmatrix} \tag{26}$$

When the composite is loaded in compression in the x_2 and x_3 directions, significant fiber tensile stresses (σ_{11f}) are induced. For instance, the tensile stress in

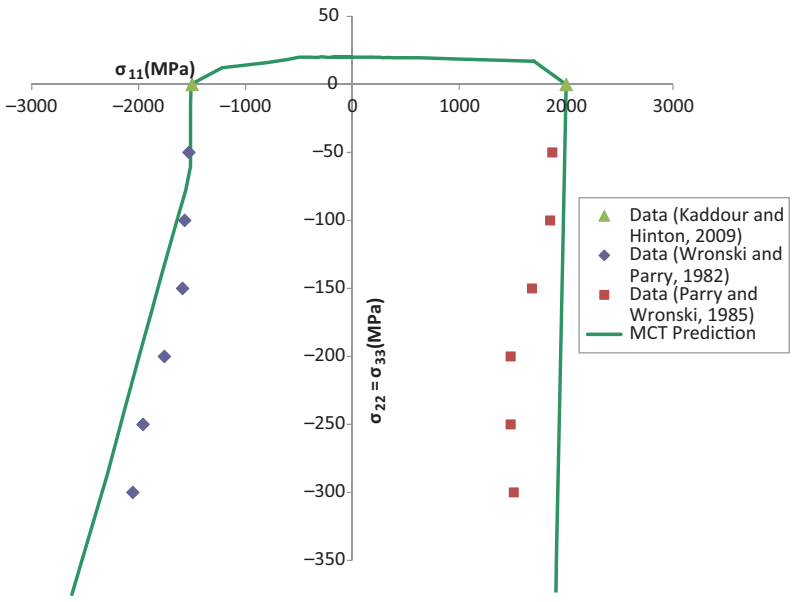

Figure 11. Test case 7; biaxial (σ_{11} versus σ_{33} with $\sigma_{22} = \sigma_{33}$) failure envelope prediction for AS carbon/epoxy1 UD laminate with experimental data from Parry and Wronski.[10,20]
UD: unidirectional.

the fibers in equation (26) is a remarkable 43% of the 10 MPa applied stress in the x_2 and x_3 directions, *despite there being no axial load*. As a result, as the transverse compressive stresses σ_{22} and σ_{33} increase in magnitude, fiber tensile stresses also increase and it takes less axial composite stress to reach the fiber failure load. This phenomenon is an excellent example of the additional insight gained in an MCT failure simulation.

The correlation of the predictions with experimental data is quite strong as the theory is capturing the key characteristics of the experiments. Moreover, simply eying the data suggests a mild revision of the UD strengths in tension and compression would lead to superb correlations.

Case 7

Figure 11 shows a predicted biaxial failure envelop, σ_{11} versus σ_{33} with $\sigma_{22} = \sigma_{33}$, for an AS carbon/epoxy UD composite. Like the previous case, failure in quadrants I and II is governed by matrix failure, whereas failure in quadrants III and IV is the result of fiber failure. The bilinear response observed in quadrant III is similar to *Case 6* for a glass/epoxy composite.

Case 8

Figure 12 shows a predicted failure envelope, σ_{yy} versus σ_{zz} with $\sigma_{zz} = \sigma_{xx}$, for a $\pm 35^\circ$ E-glass/MY750 epoxy laminate. Matrix failure corresponds to initial failure in all four quadrants. In compression-dominated regions of the envelope, final failure is governed by fiber failure.

In the tension-dominated portion of the envelope, matrix saturation, shown by the dashed line, is also predicted. Matrix saturation does not correspond to initial matrix failure. Rather, the following sequence of matrix behavior holds in every analysis.

1. Nonlinear matrix behavior initiates due to submicrocrack (bond rupture) accumulation.
2. Matrix failure occurs at a failure stress based on whether the lamina in question was a UD composite. This point is what we have defined as *initial* matrix failure in a multidirectional laminate.
3. The post-failure regime in a multidirectional laminate is characterized by through-thickness matrix cracks that increase in density as the loading continues. Eventually, a crack saturation point, referred to as matrix saturation, is reached where the crack density has reached a maximum.

Matrix saturation in a laminate is based on the data of Knops and Bögle.[5] In a related unpublished work we have recently completed, crack saturation has shown to correspond reasonably well to the weeping through a vessel wall. For an unlined pressurized specimen, crack saturation may correspond to final failure. However, we emphasize that matrix crack saturation does not imply fiber failure. In areas where matrix saturation has not been plotted, fiber failure occurs first.

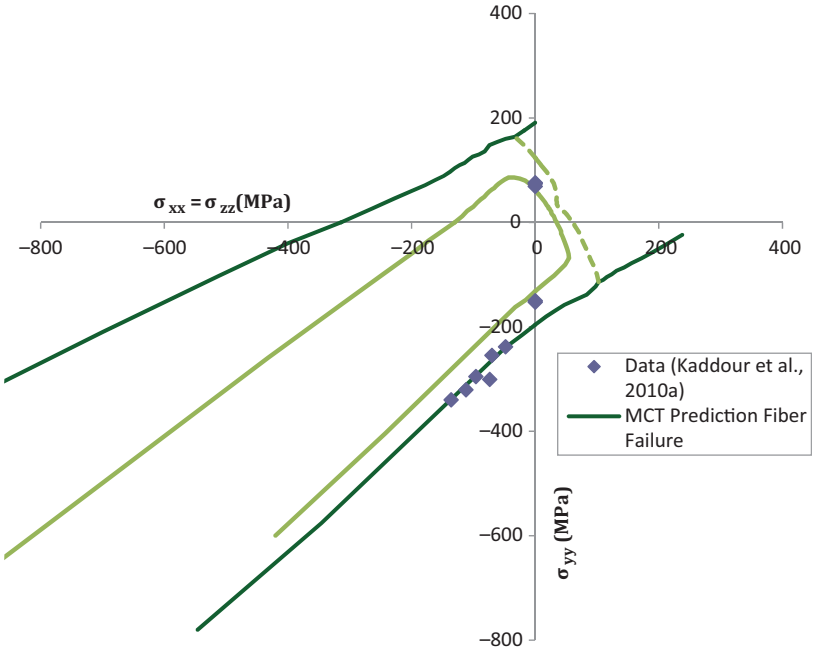

Figure 12. Test case 8; biaxial (σ_{yy} versus σ_{zz} with $\sigma_{xx} = \sigma_{zz}$) failure envelope prediction for E-glass/MY750 epoxy $\pm 35^\circ$ laminate with experimental data from Kaddour et al.[21]

The predicted failure envelope for this load case does not close in quadrant IV. However, it is conceivable that fiber failure could be predicted in the compression–compression quadrant. This load case is another example of where a more complex fiber failure criterion, allowing for an impact of transverse stresses in much the same way as the matrix failure criterion may improve on the present theory.

Case 9

Figure 13 shows a predicted stress–strain curves ε_{xx} and ε_{yy} as a function of σ_{yy} for the $\pm 35^\circ$ E-glass/MY750 epoxy laminate. As requested, the loading first consists of applying a 100 MPa hydrostatic pressure and then increasing σ_{yy} until final failure. Initial matrix failure is predicted at 250 MPa with fiber (final) failure predicted at 340 MPa.

Nonlinear behavior prior to initial matrix failure is evident in the theoretical predictions and is in excellent agreement with the experimental data. The predicted nonlinear behavior is attributed to submicrocrack accumulation. The behavior of the hoop strain ε_{xx} is particularly interesting as it starts out negative due to the applied hydrostatic pressure. As axial load increases, the hoop strain becomes positive, occurring at approximately 146 MPa in the experiment. The stress–strain prediction of this behavior occurs at 139 MPa and is in excellent agreement with the experiment.

The sharp deviation between theory and experiment at matrix failure (250 MPa) is the result of utilizing a constant secant modulus beyond this value. Enforcing a constant secant modulus is done purely for numerical efficiency. Enforcing a constant tangent modulus, while more work for an incremental theory based on total strains, would have significantly improved the results.

Case 10

Case 10 is composed of a thick section composite $(0/90/\pm 45)_S$ IM7/8551-7 carbon/epoxy laminate with layers stacked in the z-direction. The failure envelop under consideration consists of τ_{yz} versus σ_{zz} with $\sigma_{xx} = \sigma_{yy} = 0$. Failure predictions are depicted in Figure 14. Initial matrix failure, when it occurs, takes place first in the $\pm 45^\circ$ plies, then propagates to all plies. Fiber failure, where predicted, also occurs in the $\pm 45^\circ$ plies and is the result of longitudinal shear (in local coordinates) in the fibers.

In our analysis for Part A of the Exercise,[2] we misunderstood the present load case from a structural perspective in that we assumed the experiments were developed using filament wound tubes. However, on reading the data results supplied by the organizers, we understand that the tubes were machined from panels with fibers laid up in the x–y plane. Our incorrect assumption of the fabrication of the tubes requires a mild reinterpretation of the results in quadrant I. Specifically, initial matrix failure represents final failure for composite laminates loaded in through-thickness tension. Hence, in quadrant I, any reference to fiber failure or matrix saturation has been removed and the

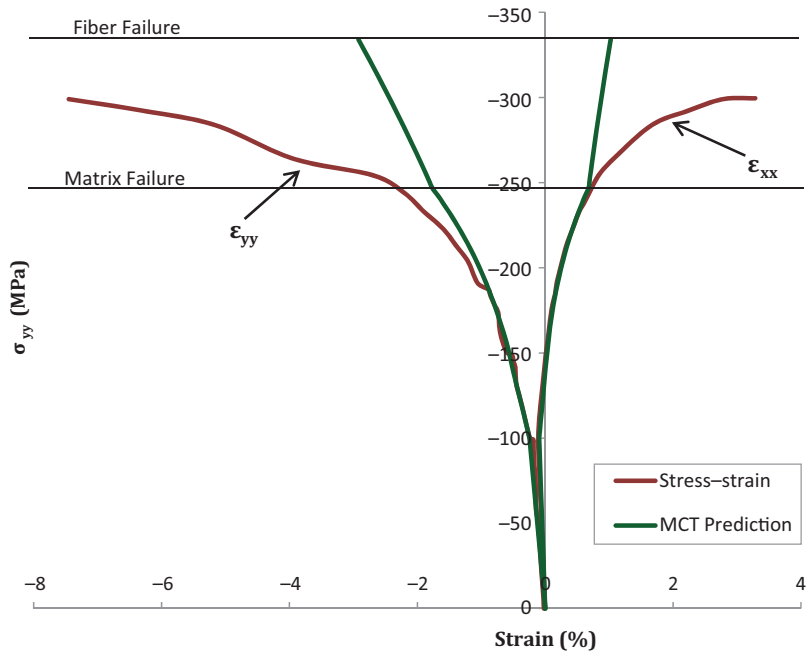

Figure 13. Test case 9; normal stress–strain curve (σ_{yy} versus ε_{xx} and σ_{yy} versus ε_{yy} with $\sigma_{xx} = \sigma_{zz} = -100$ MPa) predictions for E-glass/MY750 epoxy $\pm 35^{\circ}$ laminate with experimental curves provided by Kaddour et al.[21]

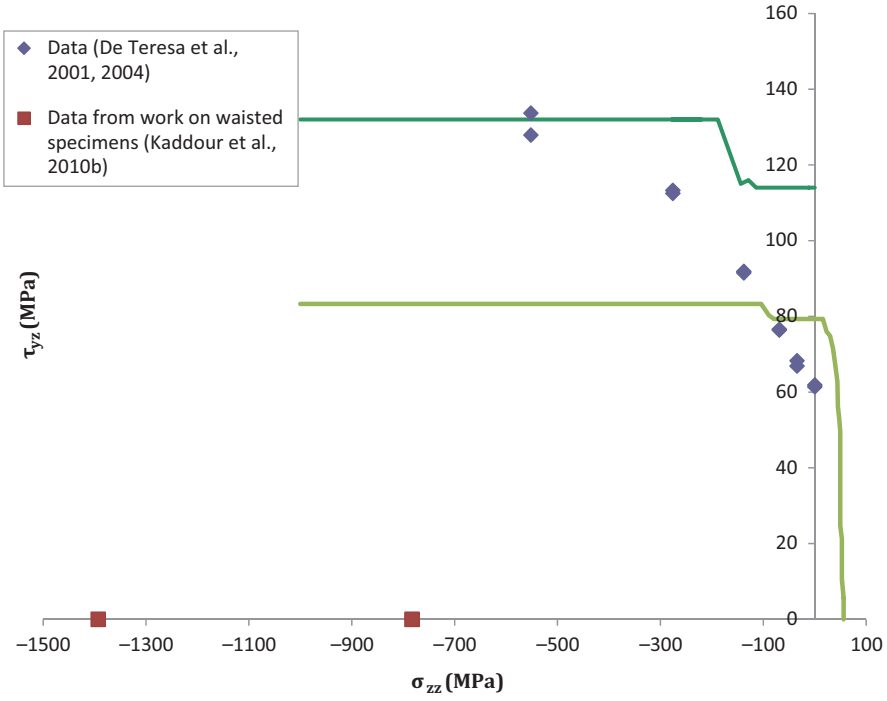

Figure 14. Test case 10; biaxial (τ_{yz} versus σ_{zz} with $\sigma_{yy} = \sigma_{xx} = 0$) failure envelope prediction for IM7/8551-7 graphite/epoxy $(0^{\circ}/90^{\circ}/\pm 45^{\circ})_S$ laminate with experimental data from De Teresa et al.[22,23]

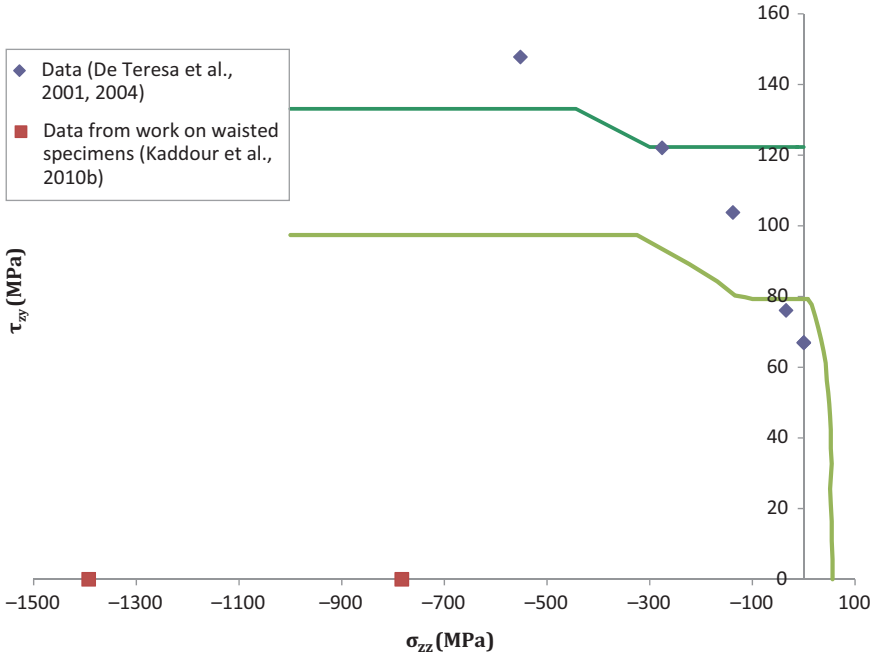

Figure 15. Test case 11; biaxial (τ_{yz} versus σ_{zz} with $\sigma_{xx}=\sigma_{yy}=0$) failure envelope prediction for IM7/8551-7 graphite/epoxy $(0^\circ/90^\circ)_S$ laminate with experimental data from De Teresa et al.[22,23]

figure submitted in Part A of the Exercise has been revised accordingly.

Our failure prediction in quadrant II generally does not do a good job of capturing the experimentally observed failure levels under through-thickness compression and shear. This result is not surprising as observations by De Teresa et al.[23] suggest that all observed failures were the result of delamination. The experimentally observed rise in shear strength as a function of increasing through-thickness compressive stress is likely the result of a combination of matrix hardening along with a suppression of delamination.

Finally, the analysis does not predict matrix failure or fiber failure due to uniaxial compression for the scale of the plot requested by the organizers. We address the possibility of ultimate failure in compression of $(0/90)_S$ laminates in our discussion of *Case 12*.

Case 11

Figure 15 shows our failure predictions for a $(0/90)_S$ IM7/8551-7 carbon/epoxy laminate. The figure shows τ_{yz} versus σ_{zz} with $\sigma_{xx}=\sigma_{yy}=0$. The data are from the same work as *Case 10* and, therefore, a similar reinterpretation of our results in quadrant I is in order. In particular, ultimate failure in the presence of through-thickness tension occurs when initial matrix failure is predicted. Hence, initial matrix failure in quadrant I corresponds to ultimate failure and any reference to matrix saturation has been removed from quadrant I of Figure 15.

Fiber failure corresponds to final failure in quadrant II of the plot. Fiber failure occurs in the 90° plies as they are subjected to a longitudinal shear load when the laminate is under an applied shear, τ_{yz}.

Case 12

Figure 16 shows predicted stress–strain curves σ_{zz} versus ε_{zz} and σ_{zz} versus ε_{xx} under transverse compression, with $\sigma_{xx}=\sigma_{yy}=0$, for a $(0/90)_S$ IM7/8551-7 carbon/epoxy laminate. The predicted response is linear elastic in appearance, due to the fact that the nonlinear pre-failure stress–strain behavior in compression was not implemented at the time of our submission for Part A of the Exercise.[2]

The analysis shown in Figure 16 was truncated at a compressive stress of 1500 MPa and failure was not predicted by the analysis at this stress level. The analysis was stopped as our interest focused on providing a stress–strain comparison for the range of experimental data available.

An estimate of failure under uniaxial compression may be achieved by performing a linear elastic MCT analysis of through-thickness compression and scaling the results until failure is predicted using the fiber and matrix constituent failure criteria. For instance, for a through-thickness composite stress of $\sigma_{zz}=-100$ MPa,

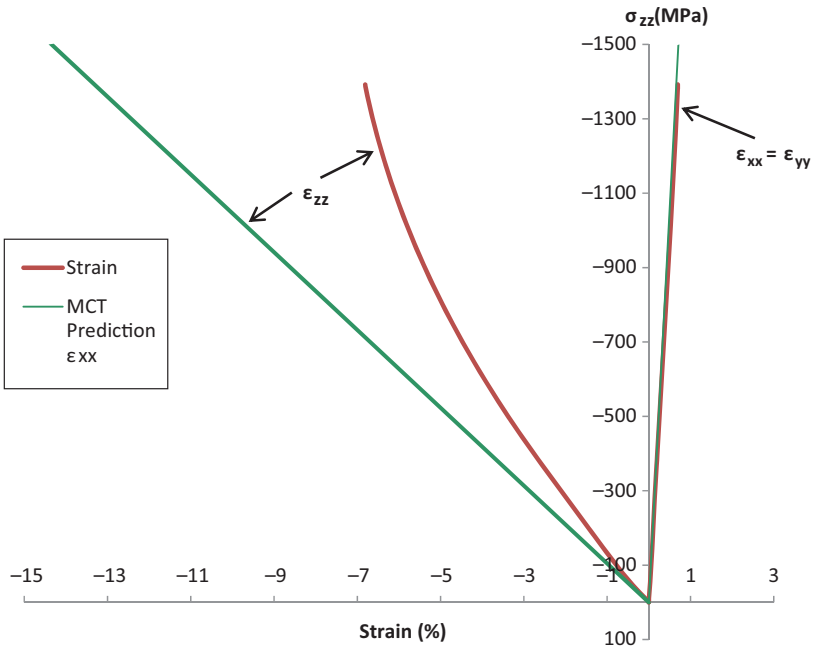

Figure 16. Test case 12; normal stress–strain curve (σ_{zz} versus ε_{xx} and σ_{zz} versus ε_{yy} with $\sigma_x = \sigma_y = 0$) predictions for IM7/8551-7 graphite/epoxy $(0^\circ/90^\circ)_S$ laminate with experimental curves provide by Kaddour et al.[24]

the constituent and composite stresses in either ply of the $(0/90)_S$ laminate are given by

$$[\sigma_f] = \begin{bmatrix} 114 & 0 & 0 \\ 0 & -39.2 & 0 \\ 0 & 0 & -105 \end{bmatrix} \text{MPa} \qquad (27)$$

$$[\sigma_m] = \begin{bmatrix} -58.7 & 0 & 0 \\ 0 & -51.8 & 0 \\ 0 & 0 & -93.2 \end{bmatrix} \text{MPa} \qquad (28)$$

and

$$[\sigma] = \begin{bmatrix} 44.3 & 0 & 0 \\ 0 & -44.3 & 0 \\ 0 & 0 & -100 \end{bmatrix} \text{MPa} \qquad (29)$$

Here, the x_3 direction is the through-thickness direction and x_1 the fiber direction.

Examination of the fiber stresses reveals the presence of a remarkably large longitudinal fiber tensile stress. The magnitude of this stress is truly surprising as it exceeds the magnitude of the applied through-thickness stress of −100 MPa. The large longitudinal fiber tensile stress occurs because of the presence of the large negative matrix stress. In fact, if we look at the composite stress, (sans MCT constituent information) the longitudinal composite tensile stress is 44 MPa and one would, we believe, not suspect the magnitude of such large *fiber* longitudinal tensile stresses.

An estimate of fiber failure of the composite can be obtained by simply scaling the linear elastic results of equation (27). We believe a linear elastic analysis represents an accurate representation of an MCT analysis prediction by the code, as nonlinearity due to compression was not enabled in the analysis we delivered. Using a fiber tensile failure of 4222 MPa, as determined from the original MCT input, the predicted failure stress is

$\sigma_{zz} = -3704$ MPa

This value is roughly 3–4 times the experimental data provided by Kaddour and Hinton.[1]

We also point out the presence of very significant compressive fiber stresses, particularly in the x_3 direction. The presence of these large stresses has no effect on the current failure criterion. This is yet another example of the merit of investigating a more advanced failure criterion for the fiber, as it is quite possible to improve the failure prediction while minimally impacting other results.

Turning our attention to matrix failure, we begin by noting that matrix failure in a continuous fiber composite is *not isotropic* at the MCT constituent level, as discussed in 'Constituent level failure criteria'. The anisotropy of the matrix failure criterion produces results that are dramatically different from a von Mises failure prediction where one might expect failure at relatively low matrix stress states. For instance, when one substitutes the matrix stress values of equation (28) into equation (8), the value of the matrix failure criterion (LHS of equation (8)) is nearly zero, −0.006 to be

precise. Hence, under through-thickness compression loading, MCT will not predict matrix failure and the fiber failure described above will be the predicted cause of ultimate failure.

Discussion

In general, we were extremely pleased with our predictions in the Exercise. We were able to capture a wide variety of unique phenomena observed in the experimental data (detailed in Ref. [25]) and, aside from a reinterpretation of our results in quadrant I in *Cases 10* and *11*, no revisions of the analysis were necessary. Our failure envelopes did not close for composite stress states that produced nearly hydrostatic compressive stress states in the matrix. This behavior is the result, in part, of one of our fundamental principles; specifically, our matrix failure criterion was designed to be independent of hydrostatic stress states. Given our lack of knowledge of experimental data, we felt our approach was a reasonable starting point. In the case of the fibers, the introduction of transverse fiber stresses appears to be a worthy endeavor that will allow failure envelops to close under large hydrostatic stresses.

In two cases (10 and 11), failure was driven by delamination, a failure mechanism that is not addressed in the failure criteria used herein. Our failure predictions in quadrant II for these cases generally do not do a good job of capturing the experimentally observed failure levels under through-thickness compression and shear. This result is not surprising as observations by De Teresa et al.[23] suggest that all observed failures were the result of delamination.

We believe that the delamination failure in *Cases 10* and *11* is driven by high transverse shear and transverse normal stresses that exist within the plies, whose peaks exist at the ply boundaries. Our modeling approach of using a single element per ply and enforcing the constraints of classical laminate plate theory (planes must remain plane) is inherently not able to capture the large stress gradients within the plies. One could model the specimen geometry and use multiple finite elements to represent the thickness of each ply. The increased resolution could potentially capture the stress gradients, thereby allowing the theory to more accurately predict the failure load.

In addition to the question of closure of failure envelopes, there remain several other areas that could benefit from further investigation. Perhaps the most pressing area requiring attention is a fundamental study of delamination and the development of appropriate failure criteria to fully capture delamination for general multiaxial stress states. Certainly, delamination is a topic that has been studied in detail, albeit, perhaps, not from a multicontinuum perspective. Improved interactive failure criteria are also areas worthy of study.

The proposed failure criteria work described above brings out an important point in that MCT is not a failure theory. Rather, it is a philosophy of predicting failure based on constituent level information. We believe the approach is ripe for failure investigations of all types, including constituent strain- and damage-based models.

Finally, it is important to examine the effects of cure stresses in *multidirectional* laminates. From an MCT perspective, a first step is to develop a viscoelastic code capable of an MCT decomposition with TTS. At present, we do not have such a capability. An appealing benefit of this study is that one could begin to explore failure at temperatures removed from a reference state, such as cryogenic applications. Such a capability does exist for UD composite laminates. No doubt, the capability of the current MCT method and those from other models employed in WWFE-II in Ref. [26], would be of a great benefit to the design community.

Again, we would like thank the organizers for allowing us to participate in both WWFE-I and WWFE-II. By posing us a set of practical problems with known data, they have immeasurably enhanced our knowledge of composite failure.

Funding

This study was sponsored by the Air Force Research Laboratory under contract no. FA 9453-07-C-0191.

Acknowledgments

The authors would like to recognize Steve Mayes who passed away in 2008. Steve was their colleague and friend, and most certainly a valued member of the composite material failure community.

Conflict of interest

None declared.

References

1. Kaddour AS and Hinton MJ. Input data for test cases used in benchmarking triaxial failure theories of composites. *J Compos Mater* 2012; 46(19–20): 2295–2312.
2. Nelson EE, Hansen AC and Mayes JS. Failure analysis of composite laminates subjected to hydrostatic stresses: a multicontinuum approach. *J Compos Mater* 2012; 46(19–20): 2461–2483.
3. Anderson EM. *An automated finite element program for micromechanics modeling of random-wavy fiber composites*. USA: University of Wyoming, 2010, MS Thesis.

4. Mayes JS and Hansen AC. Multicontinuum failure analysis of composite structural laminates. *Mech Compos Mater Struct* 2001; 8(4): 249–262.
5. Knops M and Bögle C. Gradual failure in fibre/polymer laminates. *Compos Sci Technol* 2006; 66: 616–625.
6. Mayes JS and Hansen AC. Composite laminate failure analysis using multicontinuum theory, Part A of the Worldwide Failure Exercise sponsored by DERA, Great Britain. *Compos Sci Technol* 2004; 64(3–4): 379–394.
7. Mayes JS and Hansen AC. A comparison of multicontinuum theory based failure simulation with experimental results, Part B of the World-wide Failure Exercise sponsored by DERA, Great Britain. *Compos Sci Technol* 2004; 64(3–4): 517–527.
8. Hoppel PR, Bogetti TA and Gillespie Jr JW. Literature review – effects of hydrostatic pressure on the mechanical behavior of composite materials. *J Thermoplast Compos Mater* 1995; 8: 375–409.
9. Wronski AS and Parry TV. Compressive failure and kinking in uniaxially aligned glass-resin composite under superposed hydrostatic pressure. *J Mater Sci* 1982; 17: 3656–3662.
10. Parry TV and Wronski AS. Kinking and compressive failure in uniaxially aligned carbon fibre composite tested under superposed hydrostatic pressure. *J Mater Sci* 1982; 17: 893–900.
11. Hine PJ, Duckett RA, Kaddour AS, et al. The effect of hydrostatic pressure on the mechanical properties of glass fibre/epoxy unidirectional composites. *Composites: Part A* 2005; 279–289.
12. Christensen RM. A comparative evaluation of three isotropic, two property failure theories. *J Appl Mech* 2006; 73: 852–859.
13. Kenik DJ. *Advanced techniques for constituent-based progressive failure analysis of composite structures*. USA: University of Wyoming, 2009, MS Thesis.
14. Seifert OE, Schumacher SC and Hansen AC. Viscoelastic properties of a glass fabric composite at elevated temperatures: experimental and numerical results. *Composites, Part B: Engineering* 2003; 34(7): 571–586.
15. Hinton MJ, Kaddour AS and Soden PD. The World-Wide Failure Exercise: its origin, concept and content. In: Hinton MJ, Kaddour AS and Soden PD (eds) *Failure criteria in fibre reinforced polymer composites: The World-Wide Failure Exercise*. Oxford: Elsevier, 2004, pp.2–26.
16. Shin ES and Pae KD. Effects of hydrostatic pressure on the torsional shear behavior of graphite/epoxy composites. *J Compos Mater* 1992; 26: 462–485.
17. Shin ES and Pae KD. Effects of hydrostatic pressure on in-plane shear properties of graphite/epoxy composites. *J Compos Mater* 1992; 26: 828–868.
18. Zinoviev PA and Tsvetkov SV. Mechanical properties of unidirectional organic-fiber-reinforced plastics under hydrostatic pressure. *Compos Sci Technol* 1998; 58: 31–39.
19. Zinoviev PA, Tsvetkov SV, Kulish GG, et al. Mechanical behavior of high strength unidirectional composites under 3-D state of stress. In *ICCM12*, Paris, France, 5–9 July 1999, Paper ID 1292.
20. Parry TV and Wronski AS. The effect of hydrostatic pressure on the tensile properties of pultruded CFRP. *J Mater Sci* 1985; 20: 2141–2147.
21. Kaddour AS, Soden PD and Hinton MJ. Failure of ±55 degree filament wound glass/epoxy composite tubes under biaxial compression. *J Compos Mater* 1998; 32: 1618–1645.
22. De Teresa SJ, Allison LM, Freeman OC, et al. Matrix dominated performance of thick section fiber composites for flywheel applications. *Society for the Advancement of Material and Process Engineering, 2001 Symposium*. Long Beach, CA, May 2001, pp.5–10.
23. De Teresa SJ, Freeman DC and Groves SE. The effects of through-thickness compression on the interlaminar shear response of laminated fiber composites. *J Compos Mater* 2004; 38(8): 681–697.
24. Kaddour AS, Thompson L, Li S, et al. Through thickness compressive behavior of carbon/epoxy laminates. to be published.
25. Hinton MJ and Kaddour AS. Triaxial test results for fibre reinforced composites: The Second World-Wide Failure Exercise benchmark data. *J Compos Mater* 2013; 47(6–7): 653–678.
26. Kaddour AS and Hinton MJ. Maturity of 3D failure criteria for fibre-reinforced composites: Comparison between theories and experiments: Part B of WWFE-II. *J Compos Mater* 2013; 47(6–7): 925–966.

Appendix

Notation

A	von Mises strength parameter
A_{if}	fiber failure criterion parameters ($i=1$ and 4)
A_{im}	matrix failure criterion parameters ($i=1$–5)
E_{11}, E_{22}, E_{33}	composite Young's moduli
$E_{11\beta}$, $E_{22\beta}$, $E_{33\beta}$	constituent Young's moduli ($\beta=f$ (fiber), m (matrix))
G_{12}, G_{13}, G_{23}	composite shear moduli
$G_{12\beta}$, $G_{13\beta}$, $G_{23\beta}$	constituent shear moduli ($\beta=f$ (fiber), m (matrix))
$I_{i\beta}$	constituent β transversely isotropic stress invariants ($\beta=f$ (fiber), m (matrix)); ($i=1$–5)
S_{12m}	matrix longitudinal shear stress at composite longitudinal shear failure
$+S_{11f}$	fiber longitudinal tensile stress at composite longitudinal tensile failure
V	volume
$\underset{\sim}{\varepsilon}$	composite strain tensor

$\underset{\sim}{\varepsilon}_\beta$ constituent β strain tensor ($\beta = f$ (fiber), m (matrix))

η_{Nm} matrix failure criterion excluding longitudinal shear contribution

η_{Sm} longitudinal shear portion of matrix failure criterion

σ_{ij} composite stresses referenced to the local lamina (i, $j = 1$–3) or global laminate (i, $j = x$ to z) coordinate system

$\sigma_{ij\beta}$ constituent β stresses referenced to the local lamina coordinate system ($\beta = f$ (fiber), m (matrix)); (i, $j = 1$–3)

σ_u neat resin matrix failure

$\underset{\sim}{\sigma}$ composite stress tensor

$\underset{\sim}{\sigma}_\beta$ constituent β stress tensor ($\beta = f$ (fiber), m (matrix))

ϕ_β constituent β volume fraction ($\beta = f$ (fiber), m (matrix))

$\pm$ superscript indicating the appropriate tensile or compressive value used depending on the constituent's stress state